Long-term Stability of Organic Carbon-stimulated Chromate Reduction in Contaminated Soils, and its Relation to Manganese Redox Status

Tetsu K. Tokunaga[*1], Jiamin Wan[1], Antonio Lanzirotti[2], Steve R. Sutton[2], Matthew Newville[2], and William Rao[3]

[*]Corresponding author phone (510)486-7176; e-mail: tktokunaga@lbl.gov
[1]Lawrence Berkeley National Laboratory, Berkeley, California 94720
[2]University of Chicago, Chicago, Illinois 60637
[3]Savannah River Ecology Laboratory, University of Georgia, Aiken, South Carolina 29802

Abstract

In-situ reduction of toxic Cr(VI) to less hazardous Cr(III) is becoming a popular strategy for remediating contaminated soils. However, the long term stability of reduced Cr remains to be understood, especially given the common presence of Mn(III,IV) oxides that reoxidize Cr(III). This 4.6 year laboratory study tracked Cr and Mn redox transformations in soils contaminated with Cr(VI) which were then treated with different amounts of organic carbon (OC). Changes in Cr and Mn oxidation states within soils were directly and nondestructively measured using micro X-ray absorption near edge structure spectroscopy. Chromate reduction was roughly 1st-order, and the extent of reduction was enhanced with higher OC additions. However, significant Cr(III) reoxidation occurred in soils exposed to the highest Cr(VI) concentrations (2,560 mg kg^{-1}). Transient Cr(III) reoxidation up to 420 mg kg^{-1} was measured at 1.1 years after OC treatment, followed by further reduction. Chromate concentrations increased by 220 mg kg^{-1} at the end of the study (4.6 years) in one soil. The causal role that Mn oxidation state had in reoxidizing Cr was supported by trends in Mn K-edge energies. These results provide strong evidence for long-term dependence of soil Cr oxidation states on balances between OC availability and Mn redox status.

Introduction

Chromium is among the most common metal contaminants in soils, with elevated levels of the toxic hexavalent chromate species resulting from improper disposal of wastes from a variety of industrial operations including metal plating, wood preservation, and leather tanning (1). Soils and sediments at contaminated source sites can have very high Cr concentrations, exceeding 10,000 mg kg^{-1} (2-5). Commonly occurring Cr(VI) reductants in soils are organic matter and Fe(II). Under typical ranges of subsurface pH, reduction to Cr(III) substantially decreases this metal's solubility, mobility, and toxicity (6).

The strong oxidation state dependent toxicity of Cr has prompted research and development of remediation methods that stimulate in-situ Cr(VI) reduction in contaminated soils, sediments, and groundwaters. Primarily geochemical approaches tested include injection of Fe^{2+} (7, 8), permeable reactive zero-valent Fe walls (4), and injection of H_2S (9). Biogeochemical strategies rely on supplying organic carbon (OC) to stimulate direct microbial Cr(VI) reduction and indirectly microbially mediated reduction through Fe reduction (10-14). An outstanding issue associated with redox based remediation strategies for metals is that of long-term stability of the desired nonhazardous species. For reduction based Cr remediation, the relatively high pe of Cr(VI)/Cr(III) transformations works in favor of Cr(III) stability under many conditions. However, oxidation capacities of soils vary widely. The stability of reduced

Cr in the subsurface is primarily dependent on the redox status of manganese, with Mn(IV) and Mn(III) oxides being the only common soil minerals known to oxidize Cr(III) (15-20). Soils with relatively high Mn(IV,III) oxide concentrations tend to have high Cr oxidation capacities (21, 22).

Although a wide variety of reduction-based Cr remediation strategies have been investigated in soils, the majority of tests have been carried out over the course of only a few days to months. Relatively little information is currently available on the long-term stability of reduced Cr. Insights into the long-term behavior of reductively stabilized Cr in heavily contaminated soils is particularly important to obtain because the primary human exposure pathway of concern for Cr(VI) is that of inhalation (23). In order to better understand longer-term behavior of reductively stabilized Cr, we conducted a 4.6 year laboratory environmental simulation study on Cr(VI) contaminated soil treated with varying levels of OC.

Materials and Methods

Soil. The Altamont soil (Altamont Pass, CA) used in this study is typical of many semi-arid upland areas within California. Basic properties of this Aridic Haploxerert have been described previously (24, 25). Soil from the C horizon was sieved (250 μm), and homogenized prior to bulk physical and chemical analyses. This material is calcareous (2 to 4% calcite, pH 8.3), clayey (42% clay, 52% silt, 6% sand), and contains 1% organic carbon. The native Cr concentration of this soil is 60 ± 4 mg kg^{-1}, and it has a total Mn concentration of 1,370 ± 60 mg kg^{-1}, (X-ray fluorescence analysis).

Soil columns. Several soil columns from an earlier Cr(VI) reduction study (25) were maintained for this much longer-term experiment. Six of the original 24 columns were used in the present study. Polycarbonate pipe (11.9 mm internal diameter) segments were cut into 50 mm lengths, with 30 mm by 5 mm wall sections cut away and covered with 2 layers of X-ray-transparent Kapton tape (Supporting Information, Figure S1). The inner layer of tape was cut to match the size of the wall opening, and taped to the outer layer such that the adhesive surfaces were sandwiched between Kapton films. This configuration avoided the possibility of redox reactions that could occur between soil components and the adhesive (26). Adhesive from the oversized outer layer of tape sealed the dual Kapton film windows to the polycarbonate pipe. Platinum wire electrodes were embedded along the length of each soil column for obtaining redox potential measurements (25). The columns were then packed with Altamont soil to a bulk density of 1.26 Mg m^{-3} (porosities and pore volumes of 0.52 and 1.74 mL, respectively) to a depth of 30 mm. Soils were sequentially treated with 3 different solutions. First, deionized water was infiltrated into each column to achieve a soil water content of 0.30 g g^{-1} (equivalent to 70% saturation), and incubated for 8 days at room temperature to reactivate the microbial community while maintaining aerobic conditions. Next, 3 columns each received 1.10 mL of solutions containing 1,000 mg L^{-1} Cr(VI) added as K_2CrO_4, and the remaining 3 columns received 10,000 mg L^{-1} Cr(VI). These Cr(VI) solutions were infiltrated into the soils, with the initial soil pore waters discharged out of the bottom outlet port. Upon completion of this second infiltration step, the outflow port was sealed in each column for the remainder of the experiment, such that further transport was by diffusion only. At this stage, soils contained either 4.93 or 49.3 μmol of added Cr(VI) per g soil, and the water content was 0.40 ±0.02 g g^{-1} (95 ±5% saturation). Five days after the initial exposure to Cr(VI) solutions, columns were ponded with a third solution containing various concentrations of OC. Columns received 0.60 mL (0.345 pore volume) of

tryptic soy broth as the OC remediation agent. Solutions with 0, 800, or 4,000 mg L^{-1} OC were applied to different columns, equivalent to adding 0, 9.3, or 47 μmol of OC per g soil (0, 112, or 560 μg g^{-1}). Tryptic soy broth was used as an OC source analog for decomposing plant tissue. The ponded surface of each column was capped to minimize evaporation, but vented through a segment of a hypodermic needle to maintain this boundary in equilibrium with atmospheric oxygen. Periodic uncapping for redox potential and pH measurements also help to maintain this aerated boundary condition. Soils were incubated at room temperature (21 ±2 °C), within a humidified chamber. For the longer-term incubation (greater than 1 year), soil columns were also stored in the dark, with periodic small additions of water (≈ 0.1 mL per 3 months) to compensate for evaporative loss that occurred even in the humidified enclosure.

Micro-XANES spectroscopy. Profiles of Cr and Mn oxidation states in soil columns were obtained at various times after exposure to Cr(VI) solutions, using micro- X-ray absorption near edge structure (μ-XANES) spectroscopy (27, 28). The μ-XANES measurements were obtained at beamline X26A of the National Synchrotron Light Source (NSLS, Brookhaven National Laboratory, Upton, NY), and the GeoSoilEnviroCARS beamline 13ID-C at the Advanced Photon Source (APS, Argonne National Laboratory, Argonne, IL). Large beam sizes of about 300 μm were used in order to average over a large population of mineral grains and pores. It is also worth noting that because X-ray attenuation distances in soils are around 100 μm at the Cr and Mn K-edge energies, much finer spatial resolution in these thick samples could not be obtained using smaller spot sizes. The broad beam size also helped minimize X-ray beam-induced reduction, which was observed on Cr at the brighter GeoSoilEnviroCARS beamline. By using a large spot size and keeping exposure times to less than 15 s per sample location, beam-induced Cr(VI) reduction was kept to less than 6%, as determined by repeated analyses on selected locations. No X-ray induced Cr redox changes were detectable in samples measured at beamline X26A. Mn μ-XANES spectra were only collected on these soils at X26A, where a scanning procedure described below was used to avoid beam-induced reduction.

Oxidation state standards for Cr(III) and Cr(VI) were prepared by mixing Cr_2O_3 and K_2CrO_4 into dry Altamont clays, to obtain Cr concentrations of 10,000 mg kg^{-1}. Chromium K-edge XANES spectra on these standards were collected at 0.2 to 0.5 eV steps through the pre-edge and edge regions, and 3 to 5 eV steps over the below- and above-edge regions. The energy of the pre-edge peak resulting from 1s-3d transitions allowed in tetrahedral Cr(VI) was calibrated to a value of 5,993.5 eV (29). The energy-calibrated Cr K-edge XANES spectra of the Cr(III) and Cr(VI) standards are shown in Figure 1a. Locations along the soil columns were measured with the monochromatic beam scanned below the absorption edge (5,970 to 5,988 eV, in 2 eV steps), through the pre-edge peak energy region (5,988 to 5,997 eV in 0.25 eV steps), and well above the absorption edge energy (6,170 to 6,200 eV in 5 eV steps). The background-subtracted Cr fluorescence in this latter energy range was used to normalize pre-edge peak fluorescence for calculating the Cr(VI)/[total Cr] fraction from the linear relation of Bajt et al. (30).

Manganese XANES standards consisted of $MnCO_3$ for defining the Mn(II) edge position, MnO_2 for defining the Mn(IV) edge position, and $KMnO_4$, each mixed into SiO_2 powder to about 1% Mn. The $KMnO_4$ standard was run periodically for energy calibration, with its pre-edge peak energy set equal to 6,543.3 eV (31). Examples of these Mn K-edge spectra are shown in Figure 1b. Typical Mn K-edge scans on soils were obtained with coarse steps in the below edge region (6,530 to 6540 eV, in 2 eV step), finer steps in the edge region (6541 to 6565 eV, in 0.5 eV steps), and coarse steps above the absorption edge (6,630 to 6,650 eV, in 5 eV steps). Preliminary tests showed some susceptibility for Mn redox changes under long exposures to X-

ray beams, as previously reported by Ross et al. (32). In order to avoid X-ray beam induced shifts in Mn oxidation state, most measurements on soils were done with high resolution only along the main absorption edge. This allowed quantification of Mn K-edge energies for comparison with the range bounded by Mn(II) and Mn(IV) for assessing relative Mn redox status, but does not generally quantify fractions of Mn(II), Mn(III), and Mn(IV). Local Mn redox status was characterized by determining the energy along the absorption edge corresponding to half the absorption associated with the step height (22, 33), then comparing this half-height energy to those of Mn(II) and Mn(IV) standards. Because no significant spatial trends of Mn edge energies were detected along column lengths, results were summarized as time trends of column-averaged Mn edge energies. Both Cr and Mn K-edges were scanned sequentially at 0.5 to 5 mm depth intervals along each column.

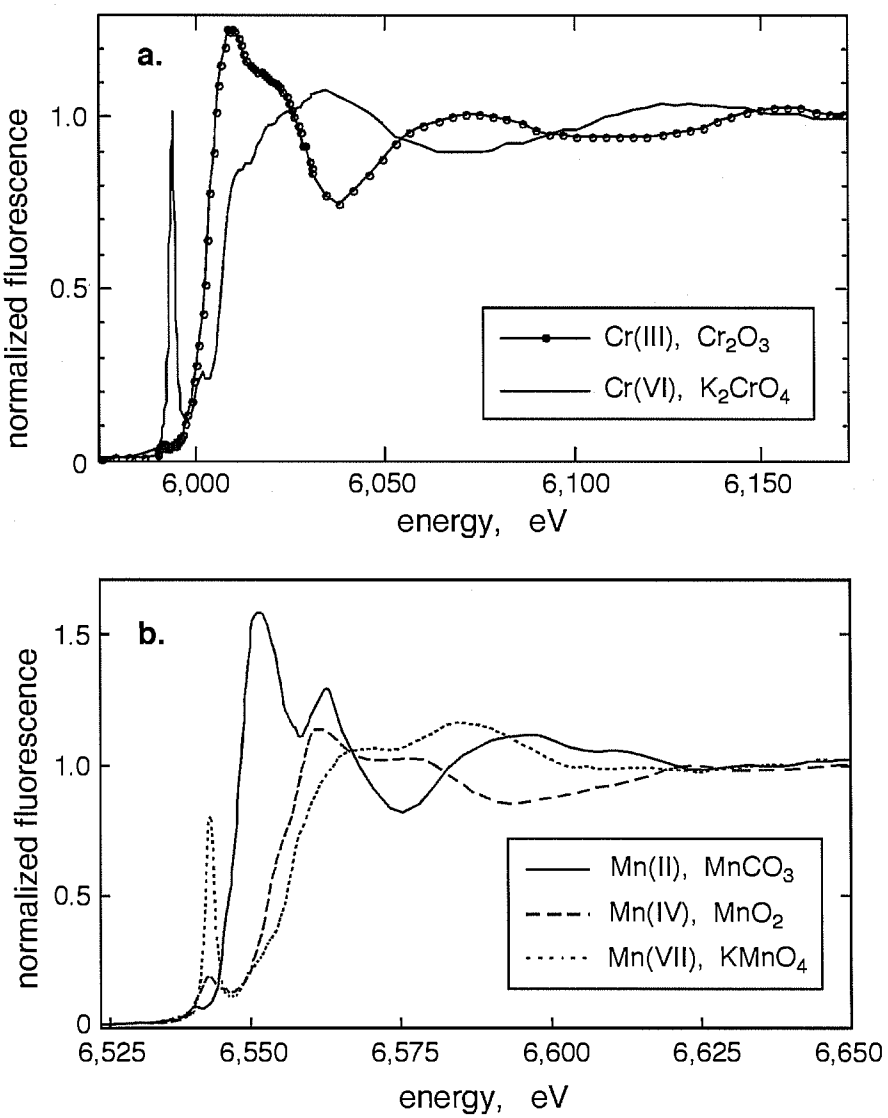

Figure 1. (**a**) XANES spectra of chromium oxidation state standards. (**b**) XANES spectra of Mn oxidation state standards.

Extractable Cr(VI) determination. At the end of the experiment (4.6 years), soil from each column was emptied, homogenized, and split into sub-samples. Half of the sub-samples were used for microbial community analyses in a companion study (Chakraborty et al., in preparation). The remaining sub-samples were analyzed for extractable Cr(VI) using the hot carbonate/hydroxide method (34) directly (wet) and after air-drying. The extraction procedure was scaled down to ≈0.8 g of soil mass because of our small sample sizes. All final extractions were normalized to an oven-dry (105°C, 24 h) soil mass basis.

Results and Discussion

General redox and pH conditions. As noted in our earlier study, redox potentials in the soils exposed to Cr(VI) remained high (0.2 to 0.5 V), and pH values were in the range of 7.2 to 7.9 (25). These redox and pH conditions persisted throughout the remainder of the experiment. It was also observed that gradients in Cr concentration and oxidation state within individual columns were insignificant at any given measurement time. Fairly homogeneous geochemical conditions continued to be observed within columns throughout the remainder of the study. For this reason, results are presented here in terms of column-averaged values of Cr and Mn oxidation states.

Chromium oxidation state changes. The normalized pre-edge peak intensity in the Cr μ-XANES spectrum provided a measure of the fraction of the local total Cr occurring as Cr(VI), regardless of phase (aqueous, sorbed, solid). Overall, Cr μ-XANES spectroscopy results showed decreases in Cr(VI) toward approximately steady-state values, or to detection limit (< 5 mg kg^{-1}). The observed trends reflect combined influences of initial Cr(VI) loading, OC addition, and oxidation of a fraction of the native soil organic carbon inventory (Figure 2). Chromate reduction occurred more rapidly and more completely with greater addition of OC, and less completely in the more heavily Cr(VI) loaded soil. Best fits to apparent first-order Cr(VI) reduction kinetics are shown in Figure 2, with parameters summarized in Table 1. Measured Cr(VI) fractions relative to their initial concentrations were least-squares fit to

$$\frac{Cr(VI)}{Cr(VI)_0} = (Cr_\infty / Cr_o) + \left[1 - (Cr_\infty / Cr_o)\right]\exp(-kt) \qquad (1)$$

where k is the effective 1st-order rate constant, t is time, and Cr_∞/Cr_0 is the steady state fraction of unreduced Cr(VI). Simple first-order Cr(VI) reduction kinetics generally describe trends in the lower Cr soils better than in the heavily Cr loaded soils (Figure 2). All of the less contaminated soils had reduction to the point that Cr(VI) was undetectable by μ-XANES (< 5 mg kg^{-1}) in 0.6 to 3 years depending on the level of OC added (Figure 2a). The fact that complete reduction was observed even without OC addition suggests that this soil has the capacity to naturally attenuate Cr(VI) up to at least 256 mg kg^{-1}. The ease with which soil organic matter reduces Cr(VI) has long been recognized, and is the basis of common assays for soil organic matter (35). In our previous work (25), Cr(VI) reduction in soils that receive no OC additions was attributed to about 3% of the native soil OC (1.0% of soil mass) that was oxidized through short-term Cr(VI) reduction reactions. However, it should be noted that the last data point from the μ-XANES analyses of the +0 OC soil is suggestive of Cr(III) reoxidation. The average final Cr(VI) concentration measured in this soil by μ-XANES spectroscopy is 8.7 mg kg^{-1} (standard deviation = 12.8 mg kg^{-1}), and this increase relative to the previously undetectable Cr(VI) levels at 3.2 and 3.7 years is weakly significant ($p = 0.25$). Although all of the soils with 256 mg kg^{-1} Cr

exposure had relatively little Cr(VI) remaining at 4.6 years, the hot carbonate extractions still released 5 to 11% of the initially applied Cr(VI) (Table 2). The higher recovery of Cr(VI) from the lower Cr soils using the hot carbonate method might have resulted from oxidation of Cr(III) during the extraction by Mn(III,IV) (36), although lower extraction efficiency was observed in our higher Cr soils. The Cr(VI) fractions directly measured by μ-XANES at the end of the experiment were lower for these soils, with the 4,000 mg L^{-1} OC treatment having no detectable Cr(VI).

Although first-order Cr(VI) reduction kinetics roughly describe overall trends in all soils, distinct departures from monotonic reduction stand out in the soils having higher Cr concentrations (Figure 2b). One major difference from approximately monotonic transformation toward complete reduction was the incomplete extent of reduction achieved in the soils exposed to highest Cr levels, even after nearly 5 years (Figure 2b). The very high concentration of Cr(VI) added (2,560 mg kg^{-1}) clearly exceeded the reduction capacity of these soils, even with addition of the highest level of OC. However, extractable Cr concentrations were less than expected based on the final μ-XANES measurements (Table 2). Conversely, as mentioned previously, more Cr was recovered in extractions of soils with lower initial Cr(VI) exposures than indicated by μ-XANES spectroscopy. Although differences between final Cr(VI) concentrations determined by μ-XANES spectroscopy and by hot carbonate/hydroxide extraction appear to depend on the level of initial Cr(VI) loading, an explanation for the disparity was not identified. The lower extraction-based recovery of Cr(VI) in the high Cr soils is especially puzzling because the hot carbonate digestion has been shown to yield good spike recoveries of very inert $PbCrO_4$ (34).

Another important variation from monotonic reduction demonstrated is Cr(III) reoxidation in the most heavily Cr-contaminated soils. In the higher Cr(VI) soils treated with 0 and 800 mg L^{-1} OC solutions, transient reoxidation of newly reduced Cr(III) was measured at 1.1 years (data points encircled by dashed lines in Figure 2b). The reoxidation amounted to increases in Cr(VI) concentrations of 260 to 420 mg $(kg\ soil)^{-1}$, and were highly significant ($p = 0.001$) in both soils. Reoxidation of Cr(III) was also measured at the end of the experiment in the high Cr soil treated with the 4,000 mg L^{-1} OC solution. Although the variability in reoxidation was larger in this last data point (standard deviation = 320 mg $(kg\ soil)^{-1}$), the increase in Cr(VI) concentration of 220 mg $(kg\ soil)^{-1}$ relative to the previous measurement at 3.8 years was also highly significant ($p = 0.001$). The apparent Cr(III) reoxidation measured at 2.26 years in the high Cr soil treated with 0 and 800 mg L^{-1} OC had weak ($p = 0.1$), and no ($p > 0.25$) statistically significant, respectively. Given the low solubilities of stable Mn(IV) oxides and precipitated Cr(III) solids, and probably minimal direct contact between these solids, other factors must be operating when Cr(III) oxidation is observed. Other studies have shown that during microbially mediated Cr(VI) reduction, significant fractions of newly reduced Cr(III) can remain in solution in organo-complexes, and thereby diffuse to Mn(IV) surfaces and reoxidize (37, 38).

241

	$Cr(VI)_0$	1^{st}-order reduction fitting			
	mg kg^{-1}	k s^{-1}	$Cr(VI)_\infty$ mg kg^{-1}	Cr_∞/Cr_0	rmsd
Low Cr, +0 OC	256	$5.7x10^{-8}$	8	0.03	0.059
Low Cr, +800 mg/L OC	256	$8.4x10^{-8}$	0	0.00	0.030
Low Cr, +4,000 mg/L OC	256	$1.3x10^{-7}$	0	0.00	0.044
High Cr, +0 OC	2,560	$1.8x10^{-8}$	1,590	0.62	0.064
High Cr, +800 mg/L OC	2,560	$1.6x10^{-8}$	1,450	0.57	0.077
High Cr, +4,000 mg/L OC	2,560	$4.6x10^{-8}$	294	0.12	0.046

242

243 **Table 1.** Fits of 1^{st}-order Cr(VI) reduction rates to time trends in soils measured by μ-XANES
244 spectroscopy. $Cr(VI)_0$ denotes the initial Cr(VI) concentration in soils, k is the effective 1^{st}-order
245 rate constant (s^{-1}), $Cr(VI)_\infty$ is the fitted steady-state Cr(VI) concentration, Cr_∞/Cr_0 is the fitted
246 steady-state relative Cr(VI) concentration, and rmsd is the root mean square deviation between
247 measured and fit Cr(VI) concentrations relative to $Cr(VI)_0$.
248

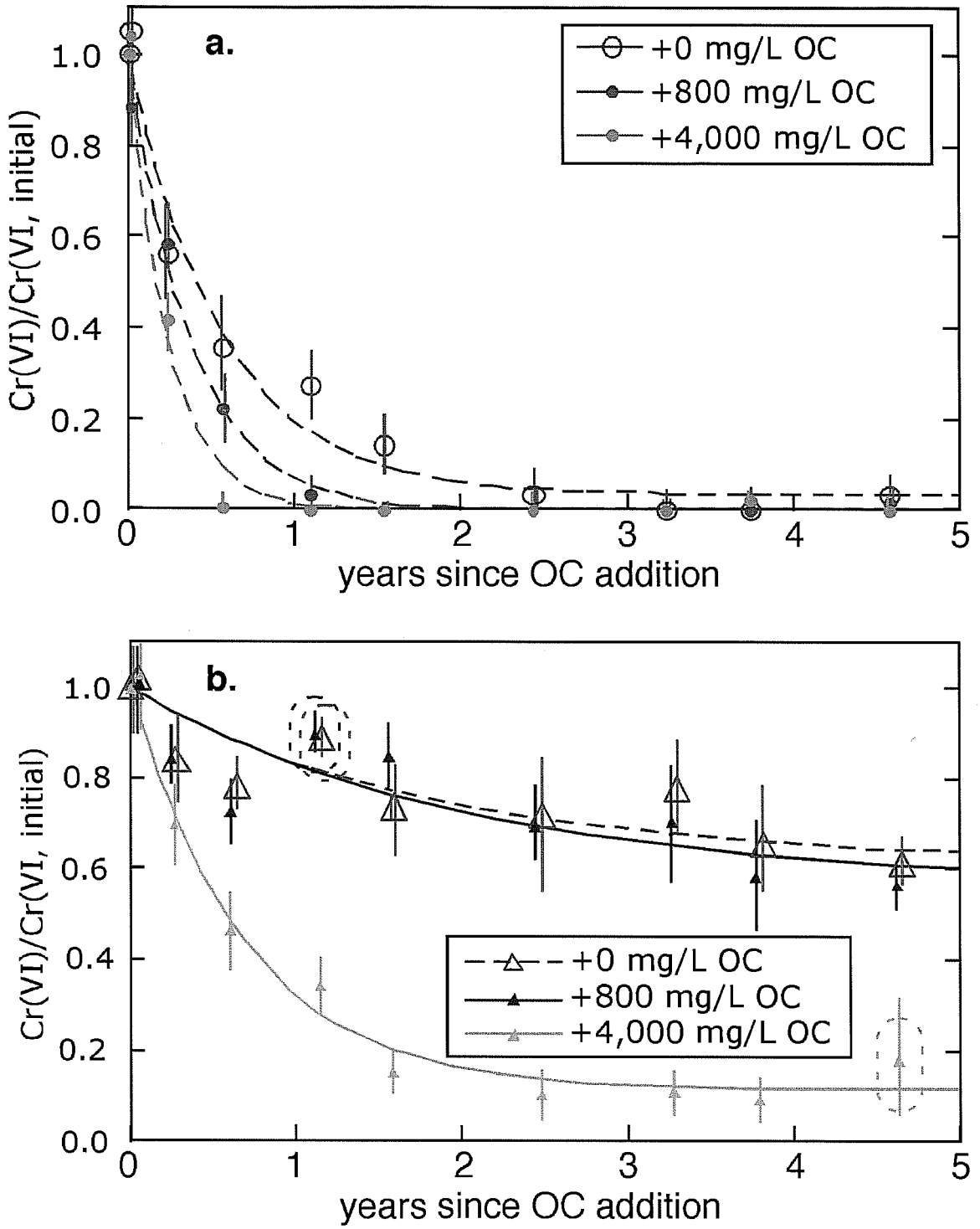

Figure 2. Time trends of Cr(VI) concentrations, relative to the initial contamination level in soils with initial Cr(VI) concentrations of (**a**) 256 mg kg^{-1}, and (**b**) 2,560 mg kg^{-1}. Data points encircled by dashed lines are for Cr(III) reoxidation significant at $p = 0.001$. Curves are least-squares fits for 1st-order Cr(VI) reduction toward final (finite or zero) concentrations.

	$Cr(VI)_O$	$Cr(VI)/Cr(VI)_O$		
	mg/kg	μ-XANES	Extract, wet	Extract, dry
Low Cr, +0 OC	256	0.03	0.07	0.07
Low Cr, +800 mg/L OC	256	0.02	0.11	0.09
Low Cr, +4,000 mg/L OC	256	0.00	0.08	0.05
High Cr, +0 OC	2,560	0.61	0.27	0.24
High Cr, +800 mg/L OC	2,560	0.57	0.24	0.22
High Cr, +4,000 mg/L OC	2,560	0.18	0.05	0.04

Table 2. Chromium (VI) fractions in soils at the end of the experiment (4.62 years), relative to initially added Cr(VI). $Cr(VI)_O$ denotes the initial soil Cr(VI) concentration. Methods used are μ-XANES spectroscopy (normalized Cr(VI) pre-edge peak height) and the hot carbonate/hydroxide extraction (applied on wet and air-dried samples).

Manganese redox changes. The possibility that soils in these columns had Mn(IV) available to reoxidize Cr(III) was examined through Mn K-edge μ–XANES measurements obtained during later stages of this study (1.5 to 4.6 years). For comparison, μ-XANES spectra were also collected on moist Altamont soil incubated over 0.9 years without exposure to Cr(VI) or additional OC. This latter sample was considered representative of Mn redox status in the original uncontaminated soil. Comparisons among all Mn K-edge spectra, despite measurements obtained at different times, was permitted through consistent calibration with the Mn(VII) pre-edge peak energy, as described previously.

Relative to the unexposed Altamont soil, the Cr-contaminated soils had Mn redox states at 1.5 years that were either significantly more oxidized or significantly more reduced (Figure 3). Most of the soils were in the group with Mn K-edge energies shifted higher than those of the original soil, indicating net Mn oxidation resulted from Cr(VI) exposure. The two soils showing greatest Mn(IV) fractions were those with high Cr that received no or intermediate levels of OC. These high Cr soils with highest Mn(IV) fractions were in fact the only soils in which Cr(III) reoxidation was detected during the previous set of Cr μ-XANES analyses (1.1 years), and exemplify the importance of tracking the redox status of both elements. The stability of reduced Cr requires supply of electron donor sufficient to also reduce Mn(IV). The one exception to the net Mn oxidation measured at 1.5 years was found in the soil that received the lower Cr(VI) exposure and highest OC input. The Mn μ-XANES spectra in that soil were shifted to significantly lower absorption edge energies, showing that the high level of added OC not only effectively reduced Cr(VI), but also reduced Mn to Mn(II). Subsequent μ-XANES measurements showed that this low Cr(VI) soil with highest OC had its Mn fully reduced to Mn(II) by 2.4 years. However, Mn in this soil gradually reoxidized back toward its original intermediate redox status. Mn μ–XANES of the low Cr soil treated with the intermediate level of OC showed a gradual reduction to Mn(II) by 3.7 years, followed by Mn reoxidation. The collective set of Mn μ-XANES measurements on all soils appears to indicate a gradual stabilization of Mn redox status toward intermediate values similar to that of the original soil. The labile nature of Mn redox status, with sensitivity to oxidation by dissolved O_2 (39) and transformations that are accelerated by microbes (40-42), will thus exert controls on long-term Cr redox cycling in soils.

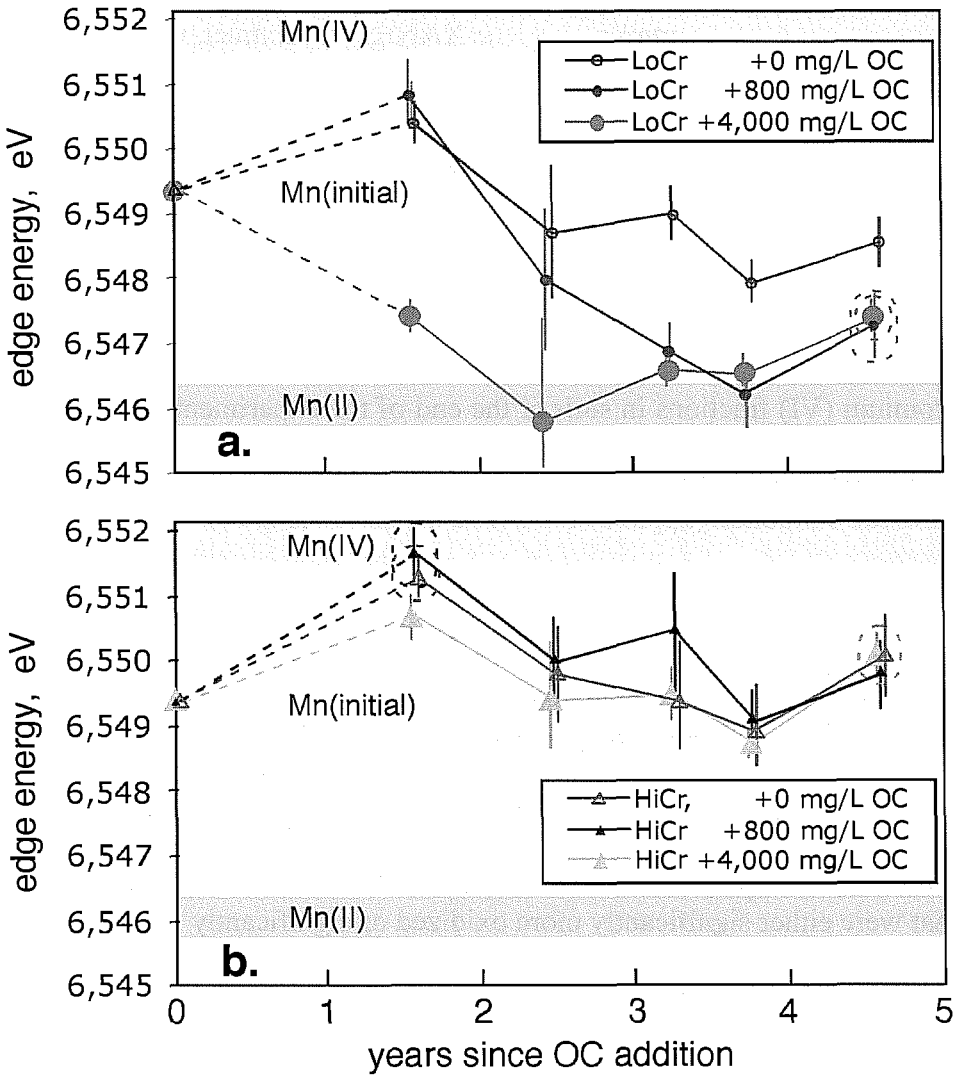

Figure 3. Time trends of Mn K-edge energies of (a.) low Cr, and (b.) high Cr-contaminated soils treated with different amounts of OC. The time zero value is for the original soil, without exposure to Cr or additional OC. Edge energies are taken at the half step height, and compared with values from Mn(II) and Mn(IV) standards. The ranges of Mn K-edge energies measured on standards and on the original soil are indicated by the vertical ranges of the horizontal bands. Error bars on data points represent ±1 standard deviation. Data points circled at 1.5 years are associated with soils that showed Cr(III) reoxidation at 1.1 years. Data points circled at 4.6 years show Mn reoxidation significant at $p = 0.001$, relative to the preceding measurement (3.8 years).

Implications for long-term stability of Cr(III). Although the transformations of Cr(VI) in contaminated soils is known to depend on Mn and available OC (6, 43, 44), this study shows that changes in redox status can exhibit reversals and require years to stabilize. Extrapolation from short-term reduction rates can yield overestimates of the extent to Cr reduction, particularly when the level of Cr(VI) contamination is high. In heavily Cr-contaminated soils, the quantities of OC or other reducing agents required to stabilize Cr(III) also need to reduce Mn(IV,III). Over

long time scales, sustained Cr and Mn reduction in soils can require a large supply of electron donor, perhaps most practically in the form of decomposing plant biomass (45). When the electron donor supply becomes limiting, Mn reoxidation back to conditions characteristic of the given soil environment can drive Cr reoxidation. When oxidizing conditions are established, a broad range of long term conditions are possible for Cr(VI) depending on prevailing biogeochemical and hydrological conditions. Possible solubility-controlling Cr(VI) phases include coprecipitates with barite (21, 46), and precipitation of chromate jarosite (47). When such solubility controls are lacking, the high capacity of Mn(IV,III) oxides to oxidize Cr(III) and releasing moderately high levels of Cr(VI) into porewaters becomes possible (48). Ultimately, magnitudes and directions of soil water fluxes will determine potential Cr exposure pathways by transporting reoxidized Cr(VI) down into underlying groundwaters or up to the soil surface.

Acknowledgments

We thank Keith Olson for technical support, and Terry Hazen (LBNL) for helpful internal review comments. Additional helpful suggestions from the anonymous reviewers and Associate Editor Janet Hering are gratefully acknowledged. Funding was provided through the Basic Energy Sciences, Geosciences Program, U. S. Department of Energy, under contract No. DE-AC03-76SF00098. Portions of this work were performed at GeoSoilEnviroCARS (Sector 13), Advanced Photon Source (APS), Argonne National Laboratory. GeoSoilEnviroCARS is supported by the National Science Foundation - Earth Sciences (EAR-0217473), Department of Energy - Geosciences (DE-FG02-94ER14466) and the State of Illinois. Use of the APS was supported by the U.S. Department of Energy, Office of Science, Office of Basic Energy Sciences, under Contract No. W-31-109-ENG-38. Portions of this work were performed at Beamline X26A, National Synchrotron Light Source (NSLS), Brookhaven National Laboratory. X26A is supported by the Department of Energy (DOE) - Geosciences (DE-FG02-92ER14244 to The University of Chicago - CARS) and DOE - Office of Biological and Environmental Research, Environmental Remediation Sciences Div. (DE-FC09-96-SR18546 to the University of Georgia). Use of the NSLS was supported by DOE under Contract No. DE-AC02-98CH10886.

Supporting Information Available

A diagram of the soil column is presented in Figure S1. This material is available free of charge via the Internet at http://pubs.acs.org.

Literature Cited

(1) Proctor, D. M.; Finley, B. L.; Harris, M. A.; Paustenbach, D. J.; Rabbe, D. *Chromium in Soil: Perspectives in Chemistry, Health, and Environmental Regulation.*; CRC Press: Boca Raton, 1997; Vol. 6.

(2) Palmer, C. D.; Wittbrodt, P. R. Processes affecting the remediation of chromium-contaminated sites. *Environmental Health Perspectives* **1991**, *92*, 25-40.

(3) Sturges, S. G. J.; McBeth, P. J.; Pratt, R. C. Performance of soil flushing and groundwater extraction at the United Chrome Superfund site. *Journal of Hazardous Materials* **1992**, *29*, 59-78.

(4) Freeman, N. C. G.; Wainman, T.; Lioy, P. J. The effect of remediation of chromium waste sites on chromium levels in urine of children living in the surrounding neighborhood. *Journal of the Air and Waste Management Association* **1995**, *45*, 604-614.
(5) Milacic, R.; Stupar, J. Fractionation and oxidation of chromium in tannery waste- and sewage sludge-amended soils. *Environmental Science and Technology* **1995**, *29*, 506-514.
(6) Rai, D.; Eary, L. E.; Zachara, J. M. Environmental chemistry of chromium. *Science of the Total Environment* **1989**, *86*, 15-23.
(7) Eary, L. E.; Rai, D. Chromate removal from aqueous wastes by reduction with ferrous ion. *Environmental Science and Technology* **1988**, *22*, 972-977.
(8) Seaman, J. C.; Bertsch, P. M.; Schallie, L. In situ Cr(VI) reduction within coarse-textured, oxide-coated soil and aquifer systems using Fe(II) solutions. *Environmental Science and Technology* **1999**, *33*, 938-944.
(9) Hua, B.; Deng, B. Influences of water vapor on Cr(VI) reduction by gaseous hydrogen sulfide. *Environmental Science and Technology* **2003**, *37*, 4771-4777.
(10) Eary, L. E.; Rai, D. Chromate reduction by subsurface soils under acidic conditions. *Soil Science Society of America Journal* **1991**, *55*, 676-683.
(11) Losi, M. E.; Amrhein, C.; Frankenberger, W. T. J. Factors affecting chemical and biological reduction of hexavalent chromium in soil. *Environmental Toxicology and Chemistry* **1994**, *13*, 1727-1735.
(12) Buerge, I. J.; Hug, S. J. Kinetics and pH dependence of chromium(VI) reduction by iron(II). *Environmental Science and Technology* **1997**, *31*, 1426-1432.
(13) Weilinga, B.; Mizuba, M. M.; Hansel, C. M.; Fendorf, S. Iron promoted reduction of chromate by dissimilatory iron-reducing bacteria. *Environmental Science and Technology* **2001**, *35*, 522-527.
(14) Bolan, N. S.; Adriano, D. C.; Natesan, R.; Koo, B.-J. Effects of organic amendments on the reduction and phytoavailability of chromate in minneral soil. *Journal of Environmental Quality* **2003**, *32*, 120-128.
(15) Eary, L. E.; Rai, D. Kinetics of chromium(III) oxidation to chromium(VI) by reaction with manganese dioxide. *Environmental Science and Technology* **1987**, *21*, 1187-1193.
(16) Johnson, C. A.; Xyla, A. G. The oxidation of chromium(III) to chromium(VI) on the surface of manganite (γ-MnOOH). *Geochimica Cosmochimica Acta* **1991**, *55*, 2861-2866.
(17) Fendorf, S. E.; Zasoski, R. J. Chromium(III) oxidation by δ-MnO_2. 1. Characterization. *Environmental Science and Technology* **1992**, *26*, 79-85.
(18) Kim, J. G.; Dixon, J., B.; Chusuei, C. C.; Deng, Y. Oxidation of chromium(III) to (VI) by manganese oxides. *Soil Science Society of America Journal* **2002**, *66*, 306-315.
(19) Bartlett, R. J.; James, B. R. Behavior of chromium in soils. III. Oxidation. *Journal of Environmental Quality* **1979**, *8*, 31-35.
(20) Weaver, R. M.; Hochella, M. F., Jr.; Ilton, E. S. Dynamic processes occurring at the Cr(III)aq-manganite (γ-MnOOH) interface: Simultaneous adsorption, microprecipitation, oxidation/reduction, and dissolution. *Geochimica Cosmochimica Acta* **2002**, *66*, 4119-4132.
(21) Kim, J. G.; Dixon, J., B. Oxidation and fate of chromium in soils. *Soil Science and Plant Nutrition* **2002**, *48*, 483-490.
(22) Negra, C.; Ross, D. S.; Lanzirotti, A. Oxidation behavior of soil manganese: Interactions among abundance, oxidation state, and pH. *Soil Science Society of America Journal* **2005**, *69*, 87-95.

(23) Rowbotham, A. L.; Levy, L. S.; Shuker, L. K. Chromium in the environment: An evaluation of exposure of the UK general population and possible adverse health effects. *Journal of Toxicology and Environmental Health, Part B* **2000**, *3*, 145-178.
(24) Tokunaga, T. K.; Wan, J.; Firestone, M. K.; Hazen, T. C.; Schwartz, E.; Sutton, S. R.; Newville, M. Chromium diffusion and reduction in soil aggregates *Environmental Science and Technology* **2001**, *35*, 3169-3174.
(25) Tokunaga, T. K.; Wan, J.; Firestone, M. K.; Hazen, T. C.; Olson, K. R.; Herman, D. J.; Sutton, S. R.; Lanzirotti, A. In situ reduction of chromium(VI) in heavily contaminated soils through organic carbon amendment. *Journal of Environmental Quality* **2003**, *32*, 1641-1649.
(26) Zavarin, M. In *Soil Science*; University of California: Berkeley, 1999; Vol. Ph. D., p 279.
(27) Bertsch, P. M.; Hunter, D. B. Applications of synchrotron-based x-ray microprobes *Chemical Reviews* **2001**, *101*, 1809-1842.
(28) Sutton, S. R.; Bertsch, P. M.; Newville, M.; Rivers, M.; Lanzirotti, A.; Eng, P. Microfluorescence and microtomography analyses of heterogeneous earth and environmental materials. In *Applications of Synchrotron Radiation in Low-Temperature Geochemistry and Environmental Science*; Fenter, P. A., Rivers, M. L., Sturchio, N. C., Sutton, S. R., Eds.; Mineralogical Society of America: Chantilly, VA, 2002; Vol. 49, pp 429-483.
(29) Peterson, M. L.; Brown, G. E., Jr.; Parks, G. A.; Stein, C. L. Differential redox and sorption of Cr(III/VI) on natural silicate and oxide minerals: EXAFS and XANES results. *Geochimica Cosmochimica Acta* **1997**, *61*, 3399-3412.
(30) Bajt, S.; Clark, S. B.; Sutton, S. R.; Rivers, M. L.; Smith, J. V. Synchrotron x-ray microprobe determination of chromate content using x-ray absorption near-edge structure. *Analytical Chemistry* **1992**, *65*, 1800-1804.
(31) Riggs-Gelasco, P. J.; Mei, R.; Ghanotakis, D. F.; Yocum, C. F.; Penner-Hahn, J. E. X-ray absorption spectroscopy of calcium-substituted derivatives of the oxygen-evolving complex of Photosystem II. *Journal of the American Chemical Society* **1996**, *118*, 2400-2410.
(32) Ross, D. S.; Hales, H. C.; Shea-McCarthy, G. C.; Lanzirotti, A. Sensitivity of soil manganese oxides: XANES spectroscopy may cause reduction. *Soil Science Society of America Journal* **2001**, *65*, 744-752.
(33) McKeown, D. A.; Post, J. E. Characterization of manganese oxide mineralogy in rock varnish and dendrites using X-ray absorption spectroscopy. *American Mineralogist* **2001**, *86*, 701-713.
(34) Vitale, R. J.; Mussoline, G. R.; Rinehimer, K. A.; Petura, J. C.; James, B. R. Extraction of sparingly soluble chromate from soils: Evaluation of methods and Eh-pH effects. *Environmental Science and Technology* **1997**, *31*, 390-394.
(35) Nelson, D. W.; Sommers, L. E. Total carbon, organic carbon, and organic matter. In *Methods of Soil Analysis. Part 3 Chemical Methods.*; Sparks, D. L., Ed.; Soil Science Society of America: Madison, WI, 1996; Vol. 5, pp 961-1010.
(36) Vitale, R. J.; Mussoline, G. R.; Petura, J. C.; James, B. R. Hexavalent chromium extraction from soils: Evaluation of an alkaline digestion method. *Journal of Environmental Quality* **1994**, *23*, 1249-1256.
(37) Buerge, I. J.; Hug, S. J. Influence of organic ligands on chromium(VI) reduction by iron. *Environmental Science and Technology* **1998**, *32*, 2092-2099.
(38) Puzon, G. J.; Roberts, A. G.; Kramer, D. M.; Xun, L. Formation of soluble organo-chromium(III) complexes after chromate reduction in the presence of cellular organics. *Environmental Science and Technology* **2005**, *39*, 2811-2817.

446 (39) Morgan, J. J. Kinetics of reactions between O_2 and Mn(II) species in aqueous solutions.
447 *Geochimica Cosmochimica Acta* **2005**, *69*, 35-48.
448 (40) Tebo, B. M.; Johnson, H. A.; McCarthy, J. K.; Templeton, A. S. Geomicrobiology of
449 manganese(II) oxidation. *Trends in Microbiology* **2005**, *13*, 421-428.
450 (41) Wu, Y.; Deng, B.; Xu, H.; Kornishi, H. Chromium(III) oxidation coupled with
451 microbially mediated Mn(II) oxidation. *Geomicrobiology Journal* **2005**, *22*, 161-170.
452 (42) Murray, K. J.; Tebo, B. M. Cr(III) is indirectly oxidized by the Mn(II)-oxidizing
453 bacterium Bacillus sp. Strain SG-1. *Environmental Science and Technology* **2007**, *41*, 528-533.
454 (43) James, B. R. The challenge of remediating chromium-contaminated soil. *Environmental*
455 *Science and Technology* **1996**, *30*, 248A-251A.
456 (44) Kozuh, N.; Stupar, J.; Gorenc, B. Reduction and oxidation processes of chromium in
457 soils. *Environmental Science and Technology* **2000**, *34*, 112-119.
458 (45) Higgins, T. E.; Halloran, A. R.; Dobbins, M. E.; Pittignano, A. J. In situ reduction of
459 hexavalent chromium in alkaline soils enriched with chromite ore processing residue. *Journal of*
460 *the Air and Waste Management Association* **1998**, *48*, 1100-1106.
461 (46) Prieto, M.; Fernandez-Gonzalez, A.; Martin-Diaz, R. Sorption of chromate ions diffusing
462 through barite-hydrogel composites: Implications for the fate and transport of chromium in the
463 environment. *Geochimica Cosmochimica Acta* **2002**, *66*, 783-795.
464 (47) Baron, D.; Palmer, C. D. Solubility of $KFe_3(CrO_4)2(OH)_6$ at 4 to 35°C. *Geochimica*
465 *Cosmochimica Acta* **1996**, *60*, 3815-3824.
466 (48) Gonzalez, A. R.; Ndung'u, K.; Flegal, A. R. Natural occurrence of hexavalent chromium
467 in the Aromas Red Sands Aquifer, California. *Environmental Science and Technology* **2005**, *39*,
468 5505-5511.
469
470